


# Morphometric Evidence for Neuronal and Glial Prefrontal Cell Pathology in Major Depression\*

View metadata, citation and similar papers at [core.ac.uk](http://core.ac.uk)

brought to you by  provided by Carolina Digital Repository

Craig A. Stockmeier

**Background:** *This report provides histopathological evidence to support prior neuroimaging findings of decreased volume and altered metabolism in the frontal cortex in major depressive disorder.*

**Methods:** *Computer-assisted three-dimensional cell counting was used to reveal abnormal cytoarchitecture in left rostral and caudal orbitofrontal and dorsolateral prefrontal cortical regions in subjects with major depression as compared to psychiatrically normal controls.*

**Results:** *Depressed subjects had decreases in cortical thickness, neuronal sizes, and neuronal and glial densities in the upper (II–IV) cortical layers of the rostral orbitofrontal region. In the caudal orbitofrontal cortex in depressed subjects, there were prominent reductions in glial densities in the lower (V–VI) cortical layers that were accompanied by small but significant decreases in neuronal sizes. In the dorsolateral prefrontal cortex of depressed subjects marked reductions in the density and size of neurons and glial cells were found in both supra- and infragranular layers.*

**Conclusions:** *These results reveal that major depression can be distinguished by specific histopathology of both neurons and glial cells in the prefrontal cortex. Our data will contribute to the interpretation of neuroimaging findings and identification of dysfunctional neuronal circuits in major depression. Biol Psychiatry 1999;45:1085–1098 © 1999 Society of Biological Psychiatry*

**Key Words:** Postmortem, neuroanatomy, frontal lobe, prefrontal cortex, neuropathology, neuroimaging

\*See accompanying Editorial, in this issue.

## Introduction

Although depressive illnesses can be serious, and even lead to suicide, nearly 80 percent of people suffering from depression can be treated successfully with medication, psychotherapy, or a combination of both. Pharmacologic, biochemical and neuroanatomical studies are beginning to establish that depressive disorders are brain diseases with unique histopathological features. Profuse neurochemical research suggests that the disruption of monoaminergic neurotransmitter pathways may be critical in the pathophysiology of major depressive disorder (MDD). In particular, the serotonin and norepinephrine systems have been implicated, because nearly all clinically effective antidepressant medications affect these neurotransmitters (Heninger and Charney 1987; Hollister and Claghorn 1993).

In contrast to the neurochemical literature, there are no systematic histopathological studies of neurons and glia on major depression or other mood disorders. Such studies may be highly relevant because reports in depressed patients and suicide victims reveal changes in monoamine receptors and transporters and related second messenger systems (Arango et al 1995; Biver et al 1997; Klimek et al 1997; Ordway et al 1994; Pacheco et al 1996; Stockmeier et al 1998) suggesting parallel cellular changes in the cortical projection areas of monoaminergic neurons. The prefrontal cortex is a particularly good candidate for a site of cellular pathology, because this region is an important target of extensive monoamine projections originating in the brainstem nuclei including the dorsal raphe, locus coeruleus and ventral tegmental area. Evidence for histopathology of glia in the subgenual region of the prefrontal cortex in major depression was recently reported by Öngür et al. (1998).

Interest in the long overlooked morphopathology of mood disorders has recently been kindled with the emergence of in vivo brain-imaging techniques. Although the results of neuroimaging studies are sometimes conflicting, the majority of such reports have implicated the prefrontal cortex as a site of functional and structural abnormalities in mood disorders (for review see Rajkowska 1997). In

Laboratory of Quantitative Neuroanatomy, Department of Psychiatry and Human Behavior, University of Mississippi Medical Center, Jackson, Mississippi (GR, JJM-H, JW, SDP); Department of Psychiatry (GD, BLR, CAS) and Department of Psychology, Case Western Reserve University, Cleveland, Ohio (JCO); and Department of Psychiatry, Vanderbilt University, Nashville, Tennessee (HYM).

Address reprint requests to Grazyna Rajkowska, Department of Psychiatry & Human Behavior, Box: 127, University of Mississippi Medical Center, 2500 N. State St., Jackson, MS 39216.

Received December 4, 1998; revised February 11, 1999; accepted February 11, 1999.

Table 1. Characteristics of Subjects

Control	Age/Gender/ Race	PMI	A-10	T F A-47	A-9	Cause of Death	Medication	Toxicology	Drugs/ Alcohol <sup>a</sup>	Family History <sup>b</sup>	
CL-1	23/F/C	11.0	22.7	22.7	22.7	Ac	levonorgestril implant	Clean	NA	NA	
CL-2	24/M/AAm	15.0	15.4	36.5	24.1	H	NA	Clean	NA	NA	
CL-3	27/F/C	15.0	20.5	21.5	20.5	N	Enalapril, Metoprolol, captopril, lopressor	Clean	NA	NA	
CL-4	30/F/C	9.0	8.9	31.6	19.4	N	NA	Clean	NA	NA	
CY-5	33/M/C	16.0	13.5	13.5	13.5	N	NA	NA	NA	NA	
CY-6	43/F/C	8.0	N/A	N/A	N/A	N	NA	NA	NA	NA	
CL-7	46/F/C	27.0	13.2	13.2	25.5	H	maxitrol?	Clean	NA	NA	
CL-8	47/M/C	17.0	7.1	7.1	6.8	N	famotidine	Clean	None	AA	
CY-9	47/M/C	12.0	7.5	7.5	7.5	N	NA	NA	NA	NA	
CL-10	58/M/C	21.5	8.8	35.0	5.0	N	digoxin, lanoxin	EtOH-gastric	None	AA,D	
CY-11	71/F/C	24.0	5.5	5.5	5.5	N	NA	NA	NA	NA	
CL-12 <sup>c</sup>	71/M/C	24.0	8.8	24.0	5.0	N	NA	Clean	AD	AA	
Average	<b>43.3</b>	<b>16.0</b>	<b>12.3</b>	<b>19.4</b>	<b>15.0</b>						
Major Depression	Age/Gender/ Race	PMI	A-10	T F A-47	A-9	Cause of Death	Medication	Toxicology	Drugs/ Alcohol <sup>a</sup>	Family History <sup>b</sup>	Duration of Depr. (years) <sup>d</sup>
CL-13	34/F/C	27.0	10.8	10.8	10.8	S	Trazodone <sup>e</sup> , alprazolam, risperidone, Amoxicillin, Valproic acid, nitrofurantoin	CO, EtOH-blood, alprazolam	NA	NA	20
CL-14 <sup>c</sup>	30/M/AAm	18.0	9.8	9.8	6.7	S	NA	EtOH-blood	AA	AD, MD, S, SA	3
CL-15 <sup>f</sup>	40/F/C	25.0	14.0	14.0	14.0	N+Ac	Temazepam, Fluoxetine, Hydrocodone, etodolac	Morphine, codeine, hydrocodone, diphenhydramine	DA	AD, D	5
CL-16	42/F/C	24.0	2.0	15.5	7.0	S	Fluoxetine, Amitrip., Paroxetine, Propoxyphene, Diazepam, Furosemide	Propoxyphene, acetaminophen	PS, DA	AD	26
CL-17	42/M/C	20.0	14.5	18.3	16.0	S	Sertraline	Sertraline, diphenhydramine, EtOH-urine, nortsertraline	None	MD, SA	0.25
CL-18	46/M/AAm	17.0	11.6	18.9	7.7	H	None	Clean	NA	SA	1
CL-19	50/F/C	23.0	23.1	16.9	14.7	S	Clomipramine, ranitidine, fluoxetine & thiothixene	Clean	None	AD, D	4
CL-20	54/M/C	23.0	6.7	12.2	12.9	Ac	Sertraline	CO, phenobarbital, phenytoin	None	AD	3
CL-21	63/F/C	24.0	6.8	12.2	6.8	N	Chlorpromazine, Clonazepam, Amitrip., amantadine	Amitrip., chlorpromazine, amantadine, lidocaine	PS, DA, AD	AD, I	30
CL-22	73/M/C	10.0	11.0	11.0	16.2	S	Nortriptyline	nortriptyline	None	None	5
CL-23 <sup>c</sup>	73/F/C	17.0	14.9	20.9	14.9	N	lithium, Nortriptyline, restoril, Clonazepam, levothyroxine	Clean	AD	AD, MD, SA	50
CL-24	86/M/C	21.0	5.6	5.6	5.6	S	Fluoxetine, Atenolol, leuprolide acetate, lupron	Clean	None	S	20
Average	<b>52.8</b>	<b>20.8</b>	<b>10.9</b>	<b>13.8</b>	<b>11.1</b>						

Table 1. Continued

A, area; AA, alcohol abuse; AAm, African American; AD, alcohol dependence; Ac, accident; C, Caucasian; D, drug abuse; DA, drug addiction; H, homicide; MD, major depression; N, natural; PMI, postmortem interval (hours)—defined as the time between death and the beginning of the formalin-fixation process; PS, polysubstance abuse; S, suicide; SA, suicide attempt; TF, time in formalin (months); NA, not available; I, institutionalized; EtOH, ethanol; Amitrip., amitriptyline.

CL, cases obtained from CWRU, Cleveland, OH.

CY, cases from the collection of Dr. P.S. Goldman-Rakic.

<sup>a</sup>Defined as psychoactive substance use disorder.

<sup>b</sup>Extended and immediate family.

<sup>c</sup>The two subjects with MDD previously met diagnostic criteria for alcohol abuse at 2 and 8 years prior to death.

<sup>d</sup>The duration of illness covers the time between the first display (and not necessarily diagnosis) of symptoms of a depressive illness and the date of death.

<sup>e</sup>Capitalized drugs were prescribed in last month of life.

<sup>f</sup>Recurrent MD, in full remission.

major depression at least two different regions, the dorsolateral prefrontal cortex (dlPFC) and the orbitofrontal-ventral region have been implicated. For example, patients with MDD consistently have reduced glucose metabolism in the left dlPFC (Baxter et al 1989; Bench et al 1993; Biver et al 1994). Decreased brain metabolism was found recently in dlPFC as well as in orbitofrontal cortex (ORB) in patients with a relapse in depression induced by depletion of tryptophan (Bremner et al 1997). Abnormally decreased metabolic activity was also localized in the ventromedial subgenual region of the frontal lobe in MDD and bipolar disorder (Drevets et al 1997). In contrast, earlier studies report increased metabolism or blood flow in orbitofrontal and ventrolateral prefrontal regions in MDD patients (Biver et al 1994; Buchsbaum et al 1986; Drevets and Raichle 1992), although blood flow tended to be lower in subjects with the greatest severity of depression (Drevets et al 1992). These apparent inconsistencies found in the orbitofrontal/ventral region indicate either the existence of different metabolic patterns in specific subareas of this region or imprecise anatomical localization of the observed changes.

Pathology of cortical cells may be related to the recent neuroimaging findings in patients with mood disorders. A 7% reduction of the total volume of the frontal lobe was reported in MDD (Coffey et al 1993) and substantial 39–48% decreases in the subgenual prefrontal gray matter volume were found in patients with MDD and bipolar depression (Drevets et al 1997). The specific neuronal and glial pathology underlying these gross morphological changes has not been determined to date. The present study is the first attempt to use state-of-the-art morphometric methods to test whether neuronal or glial cell pathology can be identified in ORB or dlPFC regions. We also tested whether the pattern of specific cortical pathology is similar or different between prefrontal regions as suggested by the neuroimaging studies.

## Methods and Materials

### Human Subjects

Human postmortem brain tissues were obtained at autopsies performed at the Cuyahoga County Coroner's Office in Cleveland, OH. Retrospective psychiatric assessments were established at Case Western Reserve University, Cleveland, OH in accordance with Institutional Review Board policies and written consent was obtained from the next-of-kin. Dr. P.S. Goldman-Rakic (Yale University School of Medicine) generously donated additional tissues from four control brains originally obtained from the University of Zagreb, Croatia, by courtesy of Dr. I. Kostovic. In all cases, a retrospective psychiatric assessment was used for establishing psychiatric histories of decedents based on information obtained from significant others or first degree family members and medical records, where available. Information pertaining to both current and lifetime psychiatric symptoms was gathered using the Schedule for Affective Disorders and Schizophrenia: Lifetime Versions (SADS-L) (Spitzer and Endicott 1978), as described by Stockmeier et al (1998). Diagnoses for major depression syndromes were based on the criteria reported in the Diagnostic and Statistic Manual of Mental Disorders-Revised (DSM-III-R) (American Psychiatric Association 1987). Consensus on diagnosis was derived during a group meeting of a psychiatrist (H.M. or B.R.) and a clinical psychologist (J.O.) after all available information had been thoroughly reviewed. Kelly and Mann (1996) have shown that there is good agreement between informant-based retrospective psychiatric assessments of deceased subjects and diagnoses by clinicians treating the same subjects before their deaths. In addition, information was obtained about previous hospital medical records, prior medical or substance abuse problems and toxicology reports. Subjects were excluded from the study if there was any evidence of head trauma, neurologic disease or a current psychoactive substance use disorder (within the last year of life). Brains were used from subjects who were younger than 73 years of age (except one subject, CL24 who was 86 years old), had a postmortem delay of less than 27 hours, and had a fixation time that did not exceed three years. Fixation times for each block of tissue are listed in Table 1.

### Tissue Sampling

Tissues were collected from the left prefrontal regions in the brains of 12 subjects retrospectively diagnosed with MDD (nonpsychotic) and 12 psychiatrically normal controls each matched by age (no more than 9 years difference between the subjects of each matching pair), gender, race, postmortem delay, and fixation time (see Table 1). Morphometric parameters (cortical thickness, cell density and cell size) were collected from two orbitofrontal regions, rostral (rORB) and caudal orbitofrontal (cORB) cortex and from the dorsolateral prefrontal cortex (dlPFC; Brodmann's area 9) (Figure 1). In addition, in the middle orbitofrontal cortex only cortical thickness was measured. The human orbitofrontal cortex has been subdivided in our recent cytoarchitectonic study into several discrete cortical regions based on differences in cellular architecture (Rajkowska et al 1998a). The most rostral subdivision of the orbitofrontal cortex is located on the lower bank of the frontomarginal sulcus, possesses mixed cytoarchitectonic features of Brodmann's area 10 and area

47, and was designated as transitional area 10-47 (Figure 1). The middle orbitofrontal cortex covers the medial wall of the orbital sulcus and constitutes area 47<sup>2</sup>. The caudal orbitofrontal cortex covers the lateral wall of the orbitofrontal sulcus, constitutes the fourth subdivision of Brodmann's area 47 and is called area 47<sup>4</sup>. The precise location and extent of dorsolateral prefrontal area 9 has been described previously based on quantitative cytoarchitectonic criteria (Rajkowska and Goldman-Rakic 1995a, b).

Blocks of tissue (3 × 3 cm) sampled from each of the three left prefrontal regions were embedded in celloidin, cut into 40 μm thick coronal sections and stained for Nissl substance. In each region selected for counting, three cortical probes spanning the entire gray matter were evenly spaced at 800 μm intervals representing different rostra-caudal levels of the areas of interest.

### 3-D Cell Counting

Computer-assisted image analysis with 3-dimensional cell counting capabilities was used to estimate neuronal and glial cell parameters (Williams 1989; Williams and Rakic 1988). This system is based on the optical disector method (Gundersen 1986) and allows for the estimation of the number of cells independent of cell shape. Neuronal and glial cell densities are expressed as number of cells/(mm<sup>3</sup> × 10<sup>-3</sup>), cell sizes are calculated as an equivalent diameter-circle, i.e., (4 × area)/circumference, of the soma size (corresponding in the case of Nissl stained glial cells to glial nuclei), and cortical thickness is measured as the distance between the overlying pia and underlying white matter. Neurons were divided into 4 classes according to their size. The range of sizes included in each class was determined for each layer using the mean (M) and the standard deviation (σ) of the control cases as follows: small (smaller than M-1σ), medium (M-1σ to M), large (M to M + 1σ) and extra large (larger than M + 1σ) (for further details see Rajkowska, 1998b). The morphometric parameters were measured in three cortical probes sampled as mentioned above. Each probe consisted of an uninterrupted series of three-dimensional counting boxes (90 × 60 × 25 μm), optically defined by the computer software. These boxes spanned the entire depth of the cortex from the overlying pial surface to the underlying white matter (Figure 1, for further details on the method, see Rajkowska et al 1998b; Selemon et al 1995). This sampling method allowed us to measure 4000–7000 neurons per given area per group and 7000–12000 glial cells per area/per group, for a total of 33,407 neurons and 58,320 glial cells measured for the study. All brains used for the study were coded and counted by two independent researchers (G.R. and J.W. or J.W. and J.J.M.H.) who were unaware of the diagnoses of the subjects.

### Statistical Analyses

Three separate statistical analyses were conducted. 1) The mean values from four morphometric parameters (neuronal density, glial density, cortical thickness and mean cell soma size) measured across all cortical layers and obtained from the three cortical probes were compared between the depressed and control groups for each cortical region separately using single factor (disease) analyses of variance (ANOVA, *p* < .05); 2) laminar differences between groups in each of the above men-

tioned parameters (analyzed separately), for each of the cortical region were analyzed using a repeated measures (six cortical layers or five sublayers) ANOVA followed by selected contrast analyses (*p* < .05; Systat 5.2.1); 3) differences between the groups in the density of different cell-size classes (small, medium, large and extra large) analyzed separately for neuronal and glial cells were compared by a repeated measures (cell-size classes) ANOVA followed by selected contrast analyses (*p* < .05). In addition, multiple correlation analysis was used to examine the influence of age, gender, postmortem delay, storage time in formalin, and duration of illness on cortical thickness, neuronal and glial densities, and soma sizes (*p* < .01). In addition, Pearson correlation matrixes were used to establish the relationship between neuronal and glial size and the density of size classes for each cortical layer and between layers.

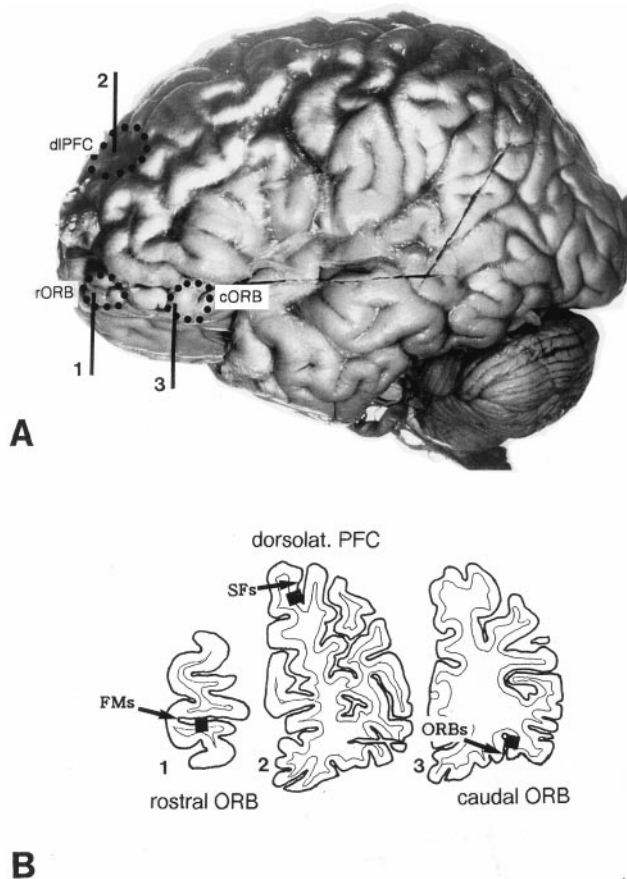


Figure 1. Localization of the three prefrontal regions from which postmortem tissues were sampled for the study. (A) Photograph of the lateral view of the left cerebral hemisphere from a healthy control. (B) Camera lucida drawings of representative coronal sections taken from each of the three studied regions. Black squares indicate cortical sites in orbitofrontal and dorsolateral prefrontal regions where measurements were taken. Abbreviations: rORB, rostral ORB; cORB, caudal ORB; dIPFC, dorsolateral PFC; FMs: fronto-marginal sulcus; SFs: superior frontal sulcus; ORBs: orbitofrontal sulcus.



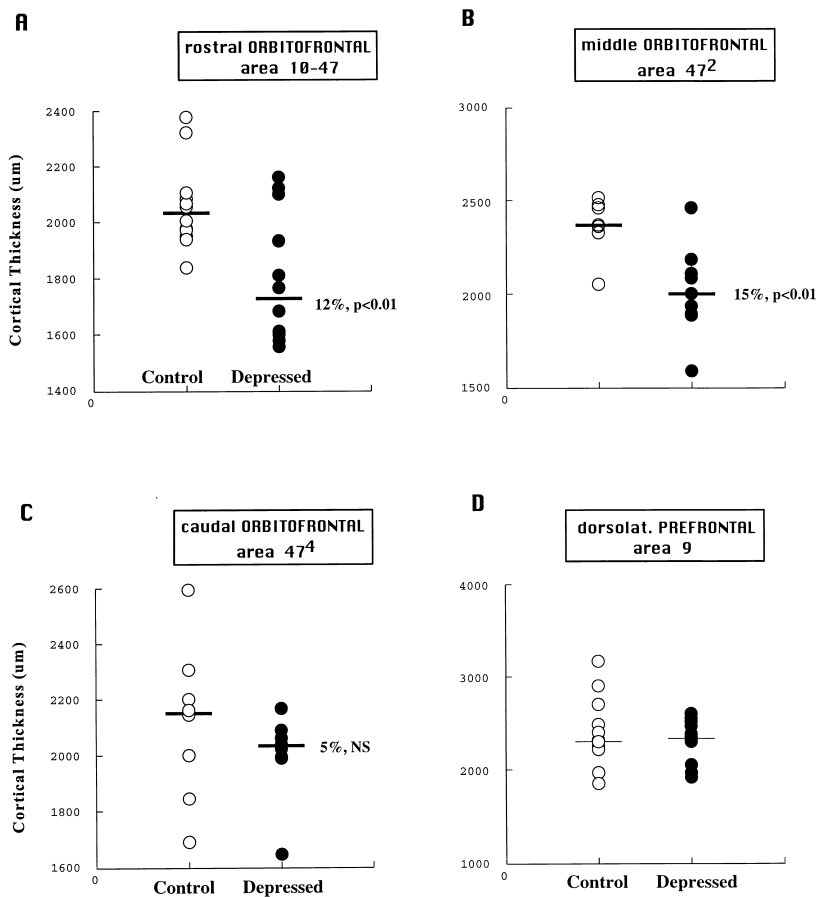


Figure 2. Plots showing the individual values of cortical thickness (measured as a distance across layers I–VI) measurements in four regions of the prefrontal cortex from control and depressed subjects. Note that there was a significant difference in cortical thickness between control and depressed groups in rostral orbitofrontal ( $n = 12$  for each group) (A) and middle orbitofrontal cortex ( $n = 8$  for each group) (B), nonsignificant trend in the caudal orbitofrontal cortex ( $n = 9$  for each group) (C), whereas no difference was found in the dorsolateral prefrontal cortex ( $n = 12$  for each group) (D).

## Results

### Rostral Orbitofrontal Cortex (area 10–47)

Our morphometric analyses in subjects with MDD showed that the overall cortical thickness of the rORB was reduced by 12% ( $F[1,22] = 10.681, p = .004$ ) as compared to normal controls (Figure 2A). These reductions in thickness were accompanied by smaller sizes of neuronal cell bodies (Figure 3). Laminar analysis of mean neuronal sizes and densities in each of the six cortical layers revealed reductions in mean neuronal size in supragranular layers (II–IIIc) of rORB in subjects with MDD (Table 2). The greatest reduction (9%) in mean neuronal size ( $F[1,22] = 23.598, p < .001$ ) occurred in layer II (Figure 3). In addition, in this layer, and in layers III and IV, the densities of the largest neurons (belonging to the “large” or “extra-large” size classes) were significantly reduced by 20–60% (Table 2). Accompanying 30–70% significant increases in the densities of small neurons were found only in layer III (Table 2).

There was a trend for a reduction in the overall glial density in rORB of subjects with MDD as compared to

controls, but these changes did not reach statistical significance ( $F[1,22] = 1.974, p = 0.17$ ; Figure 4C). Laminar analysis of size-dependent glial densities revealed significant decreases in MDD as compared to control subjects. The density of medium-sized and large glial cells was significantly reduced by 30% in layers IIIa and IV, respectively, in MDD (Table 2).

### Caudal Orbitofrontal Cortex (area 47<sup>4</sup>)

Unlike the rORB, the cORB revealed only mild (5%) and nonsignificant reductions in cortical thickness in MDD as compared to controls (Figure 2C). There was a significant reduction in mean neuronal size in layer II (6%,  $p = .035$ ), although this reduction was less prominent than in rORB. In addition, layers IIIa and Va exhibited significantly lower densities of large-size neurons in MDD (Table 3).

Glial cell density and size were prominently different in cORB in MDD as compared to controls. Significant 15% decreases in overall ( $F[1,14] = 7.645, p = .015$ ) and laminar (layers IIIc–VI) glial cell densities were evident in the diseased group (Figure 4B). These glial changes in

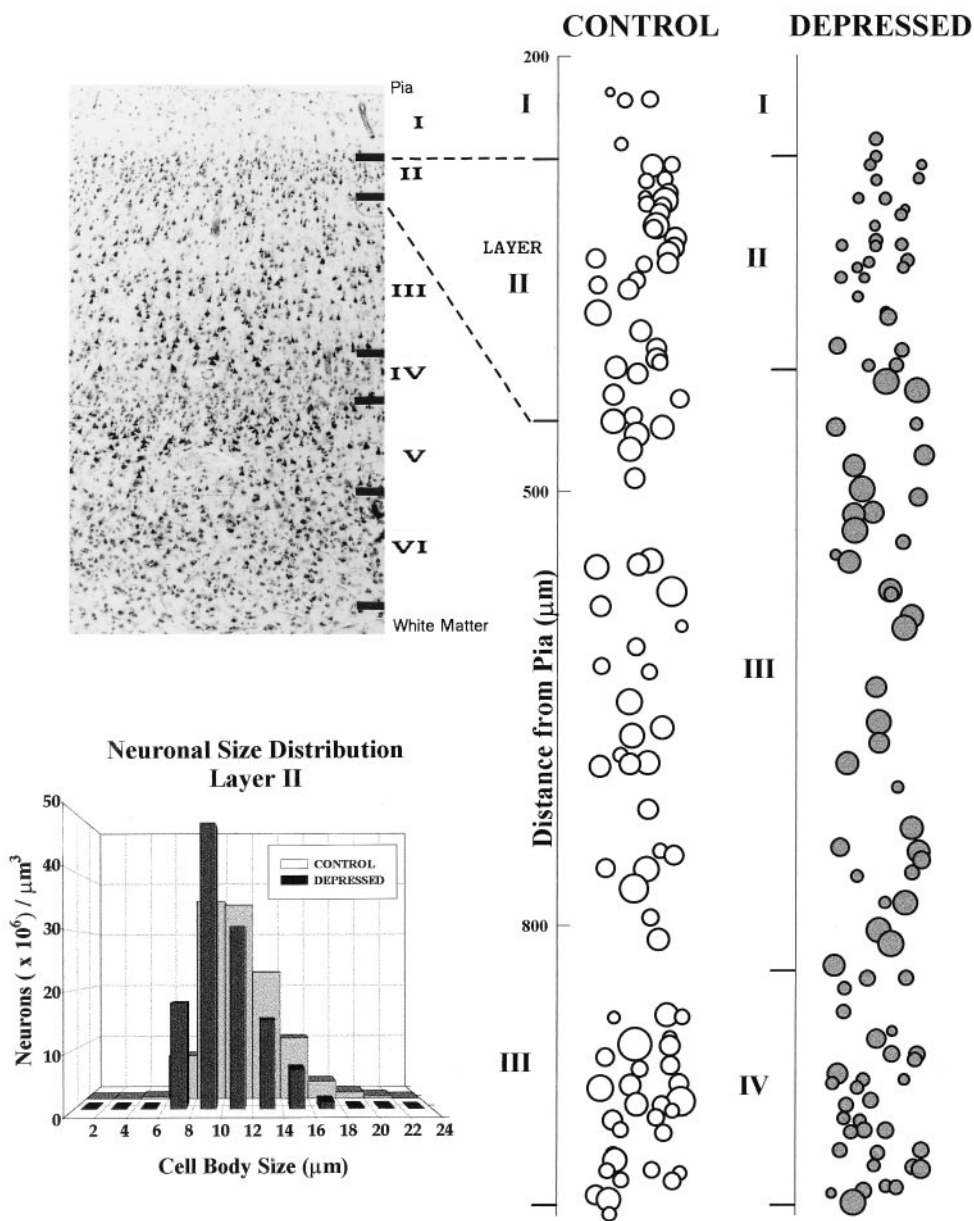


Figure 3. Changes in neuronal size and size-dependent density in layer II of rostral orbitofrontal cortex in subjects with MDD as compared to matched healthy control (both were Caucasian females, 73 and 71 years old, respectively, with postmortem delay less than 17 hours and fixation time less than 10 months). Photomicrograph of the cell composition across the six cortical layers in rORB (Upper left). Expanded print-outs of cortical layers with neuronal cell bodies represented by equivalent diameter circles with the area measured for the individual neuron in its equatorial plane (right panel). Note that in the depressed subject neuronal sizes are smaller in layers II and III than in control. Note especially dramatic increases in the density of small neurons in layer II associated with significant reductions in the density of the largest neurons of this layer (also see Table 2). This relationship is further illustrated on the histogram of the cell size distribution created for 12 MDD and 12 control subjects (lower left).

MDD were accompanied by a reduction in the density of large and medium-size glial cell nuclei predominantly in infragranular layers V and VI (Table 3, Figure 4E).

### Dorsolateral Prefrontal Cortex (area 9)

The cortical thickness of the dlPFC was nearly the same in both diseased and control groups (Figure 2D), however, there were differences evident in cell density and size between the groups. In the dlPFC, as in orbitofrontal regions, we found significant reductions in neuronal sizes in specific cortical layers in MDD. The mean size of neuronal cell bodies was decreased in MDD by 5%

( $F[1,21] = 4.838, p = .039$ ) in supragranular layer III and by 7% ( $F[1,21] = 5.666, p = .027$ ) in infragranular layer VI (Table 4). In those layers as well as in layer II the density of the largest neurons in MDD was significantly reduced by 20–60% below control values with an accompanying 40% increase in the density of the smallest neurons (Table 4, Figure 3).

The neuronal changes in dlPFC in MDD were associated with marked 20–30% reductions in the mean glial density cells in layers III and V as well as the density of medium- and large-size glial cells in those layers (Table 4, Figure 4A,D). Interestingly, in layer III, glial cells of the

Table 2. Analysis of layer-specific soma size classes, mean densities, and mean soma sizes of neurons and glia in the *rORB* in brains of control and depressed subjects

Layers	Neurons								P Values					
	Control				Depressed				Mean Neuron Density	Mean Neuron Size	Size Class Densities			
	Mean Neuron Density		Mean Neuron Size		Mean Neuron Density		Mean Neuron Size				Sm	Med	Lg	XLrg
	Avg	$\sigma$	Avg	$\sigma$	Avg	$\sigma$	Avg	$\sigma$	P	P	P	P	P	P
rORB	Avg	$\sigma$	Avg	$\sigma$	Avg	$\sigma$	Avg	$\sigma$	P	P	P	P	P	P
I	<b>24</b>	8	<b>9.2</b>	0.6	<b>22</b>	7	<b>9.0</b>	0.6						
II	<b>119</b>	16	<b>11.2</b>	0.6	<b>119</b>	15	<b>10.2</b>	0.5		<b>0.000</b> ↓			<b>0.012</b> ↓	<b>0.000</b> ↓
III	<b>63</b>	6	<b>14.3</b>	0.9	<b>60</b>	5	<b>13.5</b>	0.7		<b>0.015</b> ↓	<b>0.051</b> ↑		<b>0.011</b> ↓	<b>0.043</b> ↓
IIIa	<b>77</b>	10	<b>13.7</b>	1.3	<b>71</b>	8	<b>12.7</b>	0.8		<b>0.029</b> ↓				<b>0.017</b> ↓
IIIb	<b>53</b>	5	<b>14.6</b>	0.7	<b>51</b>	5	<b>13.9</b>	0.7		<b>0.024</b> ↓			<b>0.012</b> ↓	
IIIc	<b>71</b>	15	<b>14.4</b>	0.9	<b>69</b>	10	<b>13.5</b>	0.9		<b>0.019</b> ↓	<b>0.009</b> ↑			( <b>0.054</b> ) ↓
IV	<b>117</b>	18	<b>11.1</b>	0.5	<b>109</b>	18	<b>10.8</b>	0.5					<b>0.009</b> ↓	
V	<b>60</b>	9	<b>13.7</b>	0.8	<b>59</b>	9	<b>13.7</b>	1.1						
Va	<b>71</b>	13	<b>13.7</b>	0.9	<b>70</b>	13	<b>14.0</b>	1.4						
Vb	<b>50</b>	7	<b>13.8</b>	1.1	<b>47</b>	9	<b>13.6</b>	0.9						
VI	<b>43</b>	6	<b>13.9</b>	1.2	<b>42</b>	7	<b>13.2</b>	0.8						
All Layers	<b>62</b>	5	<b>12.9</b>	0.6	<b>61</b>	6	<b>12.3</b>	0.5		<b>0.015</b> ↓	<b>0.035</b> ↑		<b>0.028</b> ↓	( <b>0.054</b> ) ↓
Layers	Glia								P Values					
	Control				Depressed				Mean Glia Density	Mean Glia Size	Size Class Densities			
	Mean Glia Density		Mean Glia Size		Mean Glia Density		Mean Glia Size				Sm	Med	Lg	XLrg
	Avg	$\sigma$	Avg	$\sigma$	Avg	$\sigma$	Avg	$\sigma$	P	P	P	P	P	P
I	<b>97</b>	24	<b>5.1</b>	0.2	<b>88</b>	23	<b>5.3</b>	0.4						
II	<b>96</b>	32	<b>5.3</b>	0.2	<b>76</b>	22	<b>5.5</b>	0.3						
III	<b>96</b>	18	<b>5.2</b>	0.2	<b>84</b>	19	<b>5.3</b>	0.3						
IIIa	<b>89</b>	16	<b>5.3</b>	0.1	<b>78</b>	22	<b>5.4</b>	0.3				<b>0.040</b> ↓		
IIIb	<b>92</b>	19	<b>5.2</b>	0.2	<b>83</b>	19	<b>5.3</b>	0.3						
IIIc	<b>103</b>	20	<b>5.2</b>	0.3	<b>88</b>	21	<b>5.3</b>	0.2						
IV	<b>109</b>	17	<b>5.1</b>	0.2	<b>95</b>	23	<b>5.2</b>	0.3					<b>0.004</b> ↓	
V	<b>107</b>	21	<b>5.2</b>	0.3	<b>94</b>	25	<b>5.2</b>	0.2						
Va	<b>102</b>	24	<b>5.2</b>	0.3	<b>86</b>	22	<b>5.3</b>	0.3						
Vb	<b>113</b>	22	<b>5.2</b>	0.3	<b>101</b>	31	<b>5.2</b>	0.2						
VI	<b>140</b>	22	<b>5.2</b>	0.2	<b>141</b>	22	<b>5.2</b>	0.2						
All Layers	<b>110</b>	17	<b>5.2</b>	0.2	<b>100</b>	17	<b>5.3</b>	0.2						

ANOVA significant p-values (bold) and near significant values,  $0.05 < p < 0.06$  (parentheses) are indicated. Arrows indicate the direction of change. Avg: mean values for individual cortical layers and sublayers and all layers combined;  $\sigma$ : standard deviations. Mean cell densities are described in # cells/(mm<sup>3</sup> × 10<sup>-3</sup>)  $\mu$ m. Mean cell sizes are described in 4 × (Area/Circumference)  $\mu$ m. Size classes of neurons are described as small (Range: 4.3–11.4  $\mu$ m), medium (7.1–15.7  $\mu$ m), large (8.6–20.4  $\mu$ m), and extra-large (10.2–35.5  $\mu$ m). Size classes of glia are described as small (Range: 2.2–4.7  $\mu$ m), medium (4.3–5.3  $\mu$ m), large (5.0–6.1  $\mu$ m), and extra-large (5.6–13.0  $\mu$ m).

size-class with the largest nuclei also exhibited significant 60–120% ( $F[1,23] = 8.368, p = .008$ ) increases in density in MDD.

### Correlation Analysis

Decreases in cortical thickness, neuronal size and neuronal and glial density of specific size classes revealed by our study of MDD were not dependent on age, race, postmortem delay or storage time in formalin (Figure 5C–F). There was a trend

toward negative correlation with duration of illness; however, values did not reach the level of significance. Mean neuronal size in layers II, III and IV of *rORB* in MDD however, was positively correlated with the density of extra large ( $r = .683, p < .001$  for layer II;  $r = .891, p < .001$  for layer III;  $r = .670, p < .001$  for layer IV) and large ( $r = .500, p = .003$  for layer II;  $r = .611, p = .002$  for layer IV) neurons in corresponding layers and negatively correlated with the density of small ( $r = -.851, p < .001$  for layer III;  $r = -.758, p < .001$  for layer IV) and medium-sized ( $r = -.502,$

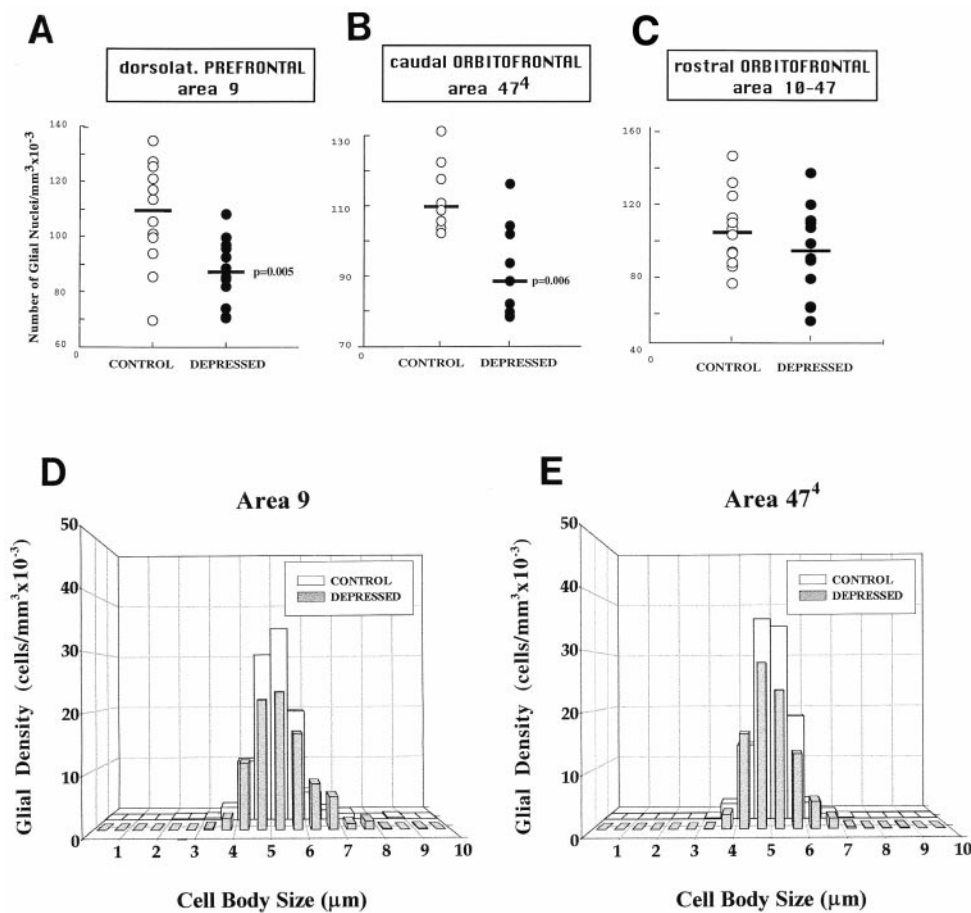


Figure 4. Plots representing individual values of the density of glial cells in layer V in three different regions of the prefrontal cortex of control and depressed subjects (A–C). Note that for areas 9 (A) and 47<sup>4</sup> (B) the density of glial cells is significantly smaller in depressed subjects compared to controls. The histograms in the bottom show the distribution of the density of glial cells somata (in our Nissl stained material corresponding to glial nuclei) into various defined size classes in areas 9 (D) and 47<sup>4</sup> (E). Note that in these areas the density of medium- and large-size glial cells is significantly decreased in depressed subjects compared to controls whereas density of glial cells with the largest nuclei is significantly increased in area 9.

$p = .012$  for layer III;  $r = -.708$ ,  $p < .001$  for layer IV) neurons in those layers (Figure 5A,B). Furthermore, the density of extra large neurons was negatively correlated with the density of small ( $r = -.665$ ,  $p < .001$ ) and medium-sized ( $r = -.615$ ,  $p = .001$ ) neurons in layer III of rORB. Thus, in MDD the smaller the mean size of the cell body, the lower the density of large and extra large neurons and the higher the density of small and medium-sized neurons.

In cORB and in dIPFC (both located caudally to rORB in the frontal lobe) the density of large or extra large neurons in MDD was also negatively correlated with the density of small neurons in layers II ( $r = -.692$ ,  $p = .002$ ) and VI ( $r = -.608$ ,  $p = .013$ ) of cORB and in layer III of dIPFC ( $r = -.586$ ,  $p = .003$ ). Moreover, the density of extra large neurons in layer II of cORB was positively correlated with the density of extra large glial cells in this layer ( $r = .631$ ,  $p = .009$ ) and with the density of large glial cells in layer I ( $r = -.645$ ,  $p = .007$ ). Finally, in MDD the densities of different size-classes of glial cells were correlated within a given cortical layer or between different layers. For example, the density of small glial cells was positively correlated with the density of medium-sized glia in layer III of rORB ( $r = .550$ ,  $p = .005$ ) whereas small glial cell density was nega-

tively correlated with the density of large ( $r = -.656$ ,  $p = .006$ ) and very large glial cells in layers II ( $r = -.819$ ,  $p < .001$ ) and III ( $r = -.601$ ,  $p = .014$ ) of cORB. Densities of large glial cells were also positively correlated between layers V and VI of cORB ( $r = .736$ ,  $p = .001$ ); densities of extra large glia were correlated between layers III and IV of rORB ( $r = .689$ ,  $p < .001$ ) and densities of small glia were correlated between layers III and IV of rORB ( $r = .864$ ,  $p < .001$ ).

#### Summary of Cellular Changes in MDD

The results described above indicate that both neurons and glial cells are involved in the histopathology of major depression in prefrontal cortex. The degree of involvement of neurons and glia in the pathology differs among prefrontal regions and specific cortical layers. Neuronal changes were most prominent in the rORB region whereas changes in glial cells were most striking in more caudally located regions of the prefrontal cortex, the cORB and dIPFC (compare Tables 2, 3 and 4). Reductions in neuronal size and density found in the rORB in MDD were restricted to supragranular layers



Table 3. Analysis of layer-specific soma size classes, mean densities, and mean soma sizes of neurons and glia in the *cORB* in brains of control and depressed subjects

Layers	Neurons								P Values					
	Control				Depressed				Mean Neuron Density	Mean Neuron Size	Size Class Densities			
	Mean Neuron Density		Mean Neuron Size		Mean Neuron Density		Mean Neuron Size				Sm	Med	Lg	XLrg
	Avg	$\sigma$	Avg	$\sigma$	Avg	$\sigma$	Avg	$\sigma$	P	P	P	P	P	P
cORB	Avg	$\sigma$	Avg	$\sigma$	Avg	$\sigma$	Avg	$\sigma$	P	P	P	P	P	P
I	<b>21</b>	9	<b>8.7</b>	0.6	<b>17</b>	6	<b>8.4</b>	0.5						
II	<b>111</b>	11	<b>10.1</b>	0.5	<b>121</b>	24	<b>9.5</b>	0.5		<b>0.035</b> ↓				
III	<b>60</b>	4	<b>14.3</b>	0.6	<b>59</b>	6	<b>13.7</b>	0.7						
IIIa	<b>83</b>	14	<b>12.6</b>	0.9	<b>76</b>	9	<b>11.9</b>	0.8					<b>0.013</b> ↓	
IIIb	<b>52</b>	5	<b>14.4</b>	0.9	<b>51</b>	8	<b>13.9</b>	0.7						
IIIc	<b>61</b>	5	<b>15.3</b>	0.8	<b>59</b>	7	<b>14.8</b>	1.2						
IV	<b>108</b>	4	<b>10.6</b>	0.5	<b>104</b>	17	<b>10.5</b>	0.4						
V	<b>56</b>	7	<b>13.6</b>	1.0	<b>54</b>	6	<b>13.6</b>	0.6						
Va	<b>73</b>	12	<b>13.6</b>	1.2	<b>67</b>	12	<b>13.7</b>	0.8					<b>0.042</b> ↓	
Vb	<b>42</b>	9	<b>13.7</b>	1.0	<b>42</b>	7	<b>13.4</b>	0.9						
VI	<b>37</b>	5	<b>13.5</b>	1.2	<b>40</b>	4	<b>13.3</b>	1.0						
All Layers	<b>57</b>	4	<b>12.6</b>	0.6	<b>57</b>	5	<b>12.2</b>	0.5						

Layers	Glia								P Values					
	Control				Depressed				Mean Glia Density	Mean Glia Size	Size Class Densities			
	Mean Glia Density		Mean Glia Size		Mean Glia Density		Mean Glia Size				Sm	Med	Lg	XLrg
	Avg	$\sigma$	Avg	$\sigma$	Avg	$\sigma$	Avg	$\sigma$	P	P	P	P	P	P
I	<b>98</b>	12	<b>5.0</b>	0.3	<b>86</b>	15	<b>5.0</b>	0.3					<b>0.034</b> ↓	
II	<b>73</b>	15	<b>5.2</b>	0.3	<b>72</b>	15	<b>5.2</b>	0.4						
III	<b>92</b>	11	<b>5.1</b>	0.2	<b>81</b>	13	<b>5.1</b>	0.2						
IIIa	<b>74</b>	7	<b>5.1</b>	0.2	<b>67</b>	13	<b>5.2</b>	0.3						
IIIb	<b>87</b>	13	<b>5.1</b>	0.2	<b>79</b>	16	<b>5.2</b>	0.3						
IIIc	<b>108</b>	17	<b>5.0</b>	0.3	<b>91</b>	17	<b>5.1</b>	0.2	<b>0.046</b> ↓					
IV	<b>110</b>	13	<b>5.0</b>	0.2	<b>90</b>	19	<b>5.0</b>	0.3	<b>0.019</b> ↓					
V	<b>110</b>	11	<b>5.0</b>	0.2	<b>89</b>	12	<b>5.1</b>	0.3	<b>0.006</b> ↓				<b>0.013</b> ↓	
Va	<b>105</b>	11	<b>5.1</b>	0.2	<b>86</b>	17	<b>5.1</b>	0.3	<b>0.047</b> ↓			<b>0.038</b> ↓		
Vb	<b>115</b>	16	<b>5.0</b>	0.2	<b>94</b>	13	<b>5.0</b>	0.2	<b>0.015</b> ↓				<b>0.003</b> ↓	
VI	<b>132</b>	18	<b>5.2</b>	0.2	<b>117</b>	10	<b>5.1</b>	0.2	<b>0.043</b> ↓				<b>0.033</b> ↓	
All Layers	<b>105</b>	7	<b>5.1</b>	0.2	<b>91</b>	14	<b>5.1</b>	0.2	<b>0.015</b> ↓				<b>0.042</b> ↓	

ANOVA significant p-values are indicated in bold. Arrows indicate the direction of change. Avg: mean values for individual cortical layers and sublayers and all layers combined;  $\sigma$ : standard deviations. Mean cell densities are described in # cells/(mm<sup>3</sup> × 10<sup>-3</sup>)  $\mu$ m. Mean cell sizes are described in 4 × (Area/Circumference)  $\mu$ m. Size classes of neurons are described as small (Range: 4.3–11.4  $\mu$ m), medium (7.1–15.7  $\mu$ m), large (8.6–20.4  $\mu$ m), and extra-large (10.2–35.5  $\mu$ m). Size classes of glia are described as small (Range: 2.2–4.7  $\mu$ m), medium (4.3–5.3  $\mu$ m), large (5.0–6.1  $\mu$ m), and extra-large (5.6–13.0  $\mu$ m).

and layer IV whereas decreases in glial cell density in MDD were found predominantly in infragranular layers of the cORB. Moreover, reductions in neuronal and glial cell density and in neuronal cell size were often found to be correlated in the same cortical layer. Significant decreases in cortical thickness in MDD were observed only in the most rostral prefrontal regions, involving rORB and middle orbitofrontal cortex (see Figure 2A, B).

## Discussion

### Cellular Changes

The densities of the largest neurons were consistently reduced in the rORB, dIPFC and, to a lesser degree, in the cORB of postmortem brains from subjects diagnosed with major depressive disorder. These decreases in densities of the largest neurons in specific layers of the rORB and dIPFC were accompanied by parallel increases in the

Table 4. Analysis of layer-specific soma size classes, mean densities, and mean soma sizes of neurons and glia in the *dIPFC* in brains of control and depressed subjects

Layers	Neurons								P Values					
	Control				Depressed				Mean Neuron Density	Mean Neuron Size	Size Class Densities			
	Mean Neuron Density		Mean Neuron Size		Mean Neuron Density		Mean Neuron Size				Sm	Med	Lg	XLrg
	Avg	$\sigma$	Avg	$\sigma$	Avg	$\sigma$	Avg	$\sigma$	P	P	P	P	P	P
dIPFC	Avg	$\sigma$	Avg	$\sigma$	Avg	$\sigma$	Avg	$\sigma$	P	P	P	P	P	P
I	<b>15</b>	4	<b>8.7</b>	0.6	<b>13</b>	4	<b>8.5</b>	0.7						
II	<b>106</b>	22	<b>10.9</b>	0.9	<b>105</b>	15	<b>10.3</b>	1.0						<b>0.043</b> ↓
III	<b>56</b>	8	<b>14.9</b>	0.9	<b>54</b>	5	<b>14.3</b>	0.7		<b>0.039</b> ↓			<b>0.020</b> ↓	<b>0.042</b> ↓
IIIa	<b>71</b>	13	<b>13.4</b>	1.3	<b>72</b>	8	<b>12.8</b>	0.7						
IIIb	<b>50</b>	9	<b>15.0</b>	0.8	<b>47</b>	4	<b>14.5</b>	0.5		(0.051)				
IIIc	<b>58</b>	13	<b>15.9</b>	1.1	<b>59</b>	8	<b>15.1</b>	1.4			<b>0.050</b> ↑			
IV	<b>106</b>	20	<b>11.3</b>	0.9	<b>103</b>	15	<b>11.0</b>	0.5						
V	<b>53</b>	7	<b>14.6</b>	1.2	<b>52</b>	7	<b>14.3</b>	0.7						
Va	<b>65</b>	10	<b>14.9</b>	1.5	<b>65</b>	7	<b>14.7</b>	0.8						
Vb	<b>42</b>	8	<b>14.5</b>	1.3	<b>42</b>	10	<b>13.9</b>	0.8						
VI	<b>36</b>	9	<b>14.5</b>	1.4	<b>38</b>	5	<b>13.5</b>	0.7		<b>0.027</b> ↓	<b>0.033</b> ↑			<b>0.033</b> ↓
All Layers	<b>54</b>	9	<b>13.4</b>	0.9	<b>53</b>	6	<b>12.8</b>	0.6		<b>0.043</b> ↓				<b>0.012</b> ↓
Layers	Glia								P Values					
	Control				Depressed				Mean Glia Density	Mean Glia Size	Size Class Densities			
	Mean Glia Density		Mean Glia Size		Mean Glia Density		Mean Glia Size				Sm	Med	Lg	XLrg
	Avg	$\sigma$	Avg	$\sigma$	Avg	$\sigma$	Avg	$\sigma$	P	P	P	P	P	P
I	<b>81</b>	21	<b>4.9</b>	0.2	<b>74</b>	15	<b>5.1</b>	0.4						
II	<b>71</b>	19	<b>5.2</b>	0.3	<b>70</b>	17	<b>5.4</b>	0.4						
III	<b>91</b>	14	<b>5.1</b>	0.2	<b>82</b>	11	<b>5.3</b>	0.3				<b>0.014</b> ↓		<b>0.029</b> ↑
IIIa	<b>76</b>	19	<b>5.1</b>	0.2	<b>68</b>	17	<b>5.4</b>	0.4		<b>0.012</b> ↑		<b>0.010</b> ↓		<b>0.008</b> ↑
IIIb	<b>90</b>	13	<b>5.1</b>	0.2	<b>80</b>	9	<b>5.3</b>	0.3	<b>0.017</b> ↓			<b>0.017</b> ↓		(0.057) ↑
IIIc	<b>103</b>	19	<b>5.1</b>	0.2	<b>93</b>	15	<b>5.3</b>	0.3						<b>0.027</b> ↑
IV	<b>107</b>	22	<b>5.1</b>	0.3	<b>94</b>	15	<b>5.3</b>	0.3						
V	<b>103</b>	13	<b>5.1</b>	0.2	<b>92</b>	11	<b>5.3</b>	0.3	<b>0.042</b> ↓			<b>0.050</b> ↓	<b>0.035</b> ↓	
Va	<b>107</b>	19	<b>5.2</b>	0.2	<b>87</b>	12	<b>5.3</b>	0.4	<b>0.005</b> ↓			<b>0.023</b> ↓	<b>0.026</b> ↓	
Vb	<b>102</b>	18	<b>5.1</b>	0.2	<b>93</b>	16	<b>5.2</b>	0.3						
VI	<b>132</b>	21	<b>5.2</b>	0.2	<b>128</b>	14	<b>5.3</b>	0.3						
All Layers	<b>100</b>	13	<b>5.1</b>	0.2	<b>92</b>	9	<b>5.3</b>	0.3				<b>0.029</b> ↓		(0.054) ↑

ANOVA significant p-values (bold) and near significant values,  $0.05 < p < 0.06$ , (parentheses) are indicated. Arrows indicate the direction of change. Avg: mean values for individual cortical layers and sublayers and all layers combined;  $\sigma$ : standard deviations. Mean cell densities are described in # cells/(mm<sup>3</sup> × 10<sup>-3</sup>)  $\mu$ m. Mean cell sizes are described in  $4 \times (\text{Area}/\text{Circumference}) \mu$ m. Size classes of neurons are described as small (Range: 4.3–11.4  $\mu$ m), medium (7.1–15.7  $\mu$ m), large (8.6–20.4  $\mu$ m), and extra-large (10.2–35.5  $\mu$ m). Size classes of glia are described as small (Range: 2.2–4.7  $\mu$ m), medium (4.3–5.3  $\mu$ m), large (5.0–6.1  $\mu$ m), and extra-large (5.6–13.0  $\mu$ m).

density of small neurons and were correlated with reductions in mean neuronal sizes. The latter observation suggests that neuronal shrinkage or a developmental deficiency rather than neuronal loss account for the overall smaller neuronal sizes in those cortical layers. If neuronal loss had occurred the density of large neurons would have been decreased without associated increases in the density of small neurons, as has been recently demonstrated in

Huntington's disease, a well-characterized neurodegenerative disorder (Rajkowska et al 1998b).

The changes in densities of large and extra large neurons in MDD were positively correlated with changes in glial cell densities. A lower density of the large neurons was accompanied by a lower density of glial cells in specific cortical layers. In the dIPFC, the lower overall glial density was accompanied by marked increases in the density of the

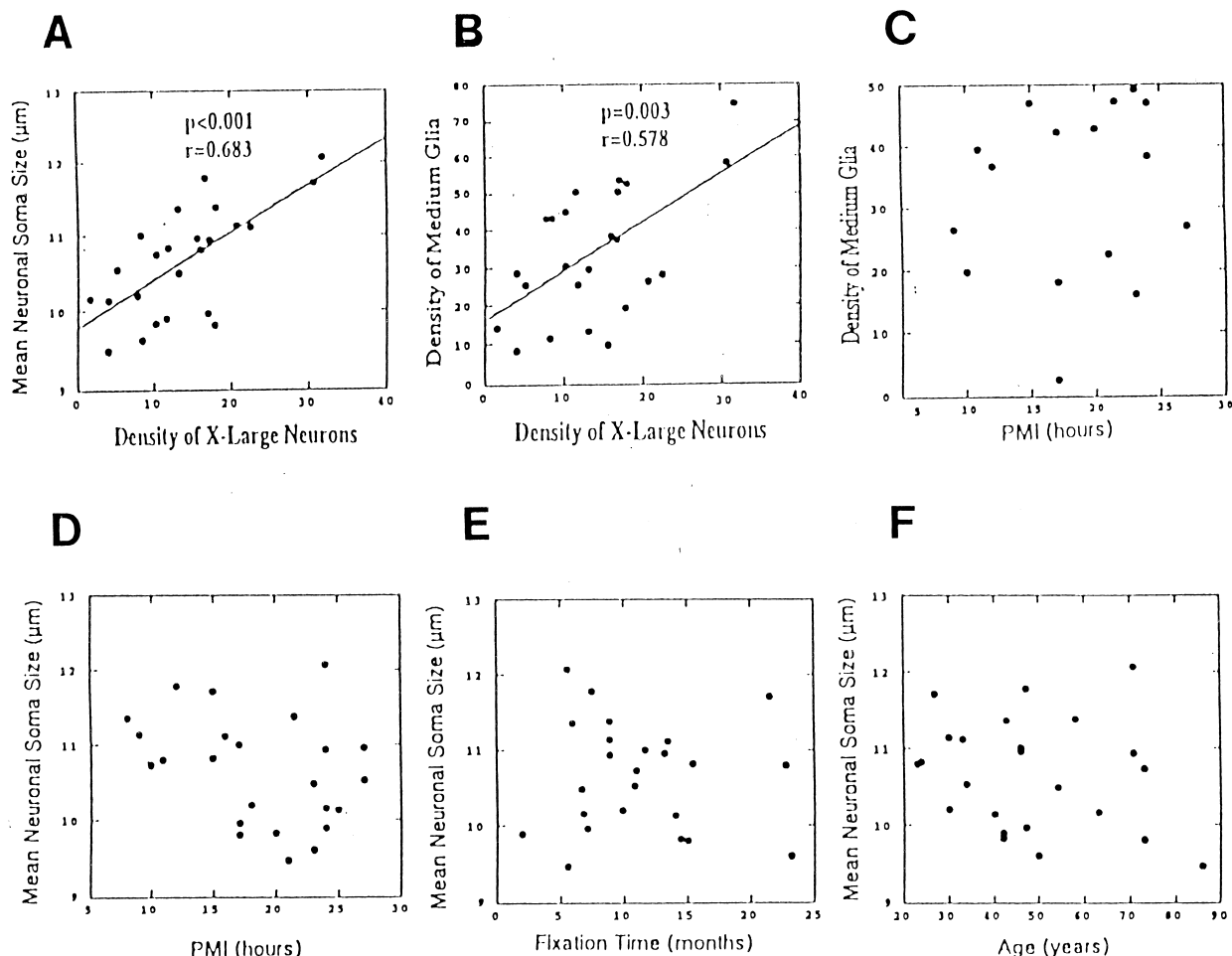


Figure 5. Plots of correlation analysis for several relevant parameters related to the brain samples used in the present study in specific layers, where significant changes were found. Plots A and B (both from layer II in rORB) show that the density of extra large neurons is positively correlated with mean neuronal soma size (A) and with the density of medium-sized glia (B). In plot C, we illustrate the absence of correlation between density of glial cells and postmortem interval in layer V of cORB, where we found the greatest changes in glial density. Plots D, E, F (all from layer II of rORB) show that the postmortem interval (PMI) (D), the time in fixative (E), and the age of the subjects (F) are not significantly correlated with mean neuronal soma size.

largest glial nuclei suggesting enlargement of the glial cells. Similar increases in glial nuclear sizes are reported in the same prefrontal region for Huntington's disease (Rajkowska et al 1998b). In Huntington's disease however, enlargement of glial cells is associated with marked increases in glial cell densities (Selemon et al 1995). Glial enlargement and proliferation in neurodegenerative brain disorders seem to occur in response to neuronal injury. Our present finding of a decrease rather than an increase in glial density in MDD seems unique to mood disorders and has not been observed in previous morphometric studies of the prefrontal cortex in subjects with schizophrenia or Huntington's disease (Rajkowska et al 1998b; Selemon et al 1995). Recently, we detected comparably lower glial densities in brain tissues from subjects with bipolar (manic-depressive) illness (Rajkowska et al 1997). Our observations on glial changes in both types of mood

disorders, MDD and bipolar illness, have been independently confirmed (Öngür et al 1998).

#### *Implications for the Link Between Cell Pathology and Neuroimaging*

The neuronal and glial changes described here suggest that different regions of the prefrontal cortex might contribute differentially to the histopathology of MDD. Significant decreases in cortical thickness and neuronal sizes in rORB in MDD suggest that atrophy of cortical neurons may account for the reduced volume of cortical gray matter and be related to the decreased metabolic activity reported for this region in neuroimaging studies on depressed patients (Bremner et al 1997). Likewise, the marked reductions in glial densities and moderate reductions in neuronal size

(without significant decreases in cortical thickness) found in the left cORB and dlPFC may be related to the altered metabolism reported in these regions. Glial cells are involved in the active processing of glucose and are reported as the primary sites of glucose uptake and phosphorylation during neuronal activity (Tsacopoulos and Magistretti 1996).

Our histopathological data therefore indicate that the two orbital regions and the dlPFC exhibit cytoarchitectural alterations involving both neurons and glial cells. The differences that we found between rostral (rORB) and caudal (cORB and dlPFC) prefrontal regions in MDD refer to the degree of neuronal or glial contribution to putative pathology of specific cortical layers in these prefrontal regions. Therefore, the present data suggest the existence of a rostral-to-caudal rather than a dorsal-to-ventral pattern of morphometric changes in the prefrontal cortex of subjects with MDD. This observation is of interest because previous computerized tomographic scans of brain lesions in depressed patients have shown that lesions in more rostral regions of the frontal pole are positively correlated with the occurrence of more severe depression (Robinson and Szetela 1981). It is tempting to speculate that the duration of depression may correlate with the degree and severity of the rostral frontal damage. In our cases a decrease in the size of neuronal somata in rORB showed a nonsignificant trend toward a negative correlation with the duration of depression. A challenging interpretation of the results that cannot be ruled out is that there is a temporal sequence in the appearance of histopathological changes in the frontal lobe that will spread through dysfunctional connections to neighboring cortical areas.

### *Laminar-Specific Cell Pathology and Neurotransmitter Systems*

The reductions in neuronal sizes described here in MDD were restricted to upper cortical layers (II–IV) in the rORB although in cORB and dlPFC other layers were also affected. The differential involvement of cortical layers suggests that specific populations of cortical neurons might be related to the histopathology of prefrontal cortex in MDD. Primate studies revealed that neurons of layers II–IV are involved in the establishment of connections with other cortical regions and are targets for subcortical inputs (Schwartz and Goldman-Rakic 1984; Selemon and Goldman-Rakic 1988). Recent findings in monkey prefrontal cortex show that serotonergic axons terminate predominantly on nonpyramidal neurons of layers I to IV (Lewis 1992; Smiley and Goldman-Rakic 1996). Moreover, layer II, where neuronal diminution was especially pronounced can be distinguished from other cortical layers of normal human prefrontal cortex by a particularly dense lamina of serotonergic receptors (Arango et al 1995; Pazos

et al 1987). Finally, the reports of an upregulation in serotonin-1A and serotonin-2A receptors and downregulation of serotonin transporters predominantly in layer II and in layers III–IV of the ventrolateral prefrontal cortex in (presumably depressed) suicide victims (Arango et al 1990; Arango et al 1995) suggest a neuropharmacological link to altered neuronal size in upper layers of this region. These morphometric and pharmacologic observations imply that serotonergic axons, and the receptors and cortical neurons that are recipients of these axons, may be important targets of antidepressant medications.

In cORB and dlPFC, in contrast to rORB, laminar-specific reductions in neuronal sizes and glial densities were found in the lower portions of layer III and in layers V and VI in MDD. From primate studies, layers III, V and VI are known to give rise to glutamatergic pathways descending to various subcortical structures, including the basal ganglia, that are involved in control of motor functions (Arikuni and Kubota 1986; Selemon and Goldman-Rakic 1985). It is interesting to speculate that altered functioning in these pathways may be related to the psychomotor retardation often observed in depressed patients. Moreover, layer V of the non-human primates and human prefrontal cortex is the site of colocalization of dopamine-1 and dopamine-2 receptors (Goldman-Rakic 1998; Goldman-Rakic et al 1990; Joyce et al 1991; Williams and Goldman-Rakic 1998) further suggesting the prefrontal involvement of dopaminergic system in the neuropathology of MDD. In addition, neurons of layers V and VI are recipients of extensive noradrenergic projections (Lewis and Morrison 1989) coming from the locus coeruleus, that is known to be involved in the pathology of MDD (Klimek et al 1997; Ordway et al 1994). Thus, the layer-specific cellular changes reported here suggest an involvement of many other neurotransmitter systems in addition to the serotonin system.

### **Conclusions**

The cellular changes described here indicate that both types of brain cells, neurons and glia, are abnormal in major depression, and may contribute to pathologic changes in the prefrontal cortex related to the psychiatric disorder. The question remains whether depressed patients are genetically predisposed for the cortical cell changes found in their brains postmortem and they were born with smaller neurons or less glia or whether the cellular changes are a consequence of MDD. Alternatively, those genetically predisposed to the greatest histopathological alterations may exhibit the most pernicious psychiatric symptoms. It would be useful to examine the morphological and metabolic features of prefrontal cortex in identical twins discordant for MDD. Interestingly, cortical layers II and III, where we observed the most profound neuronal and glial changes, are among the last prefrontal layers to develop; their neurochemical maturation



and the stabilization of their neuronal elements is prolonged beyond birth in the human prefrontal cortex (Koenderink et al 1994; Kostovic et al 1988; Mrzljak et al 1992). Of great relevance to the neurodevelopmental issue is the recent proton MRS study that found increased levels of cytosolic, choline-containing compounds in the orbitofrontal cortex of depressed adolescents (Steingard et al 1998). This study suggests that abnormal development of the orbitofrontal cortex may be associated with the early onset of depression.

The pathology of cortical cells in MDD must also be evaluated taking into consideration that those changes might be a result of exposure to antidepressant medications. It remains to be determined whether the morphological changes detected postmortem in subjects with MDD are trait or state dependent, and whether antidepressant medications have effect on cell morphology. In the present study, comparable cell pathology was detected even in the two MDD subjects who were never taking antidepressant medications. Further behavioral and morphometric studies on animals treated with antidepressant medications will shed more light on this crucial issue.

The present report represents the first morphometric evidence for the involvement of neurons and glial cells in the histopathology of major depression. These findings open new insights into the neurobiology of major depression and suggest it as a brain disease with distinct histopathological features.

---

This study was sponsored by NARSAD Young Investigators Award (GR), grants MH54710 and MH55872 (GR), The American Foundation for Suicide Prevention and MH45488 (CAS). We are grateful to G. Bissette, Ph.D. for valuable comments on the manuscript and to W. Page and M. Richmond for excellent technical assistance. We thank A. Halaris, M.D., Ph.D. for providing generous departmental support and P.S. Goldman-Rakic, Ph.D. and P. Rakic, Ph.D. for sharing software for 3-D cell counting. We acknowledge the outstanding assistance of the Cuyahoga County Coroner and staff from Cleveland, OH.

---

## References

- American Psychiatric Association (1987): *Diagnostic and Statistical Manual of Mental Disorders*, Revised Third Edition. Washington, DC: American Psychiatric Association.
- Arango V, Ernsberger P, Marzuk PM, Chen JS, Tierney H, Stanley M, et al (1990): Autoradiographic demonstration of increased serotonin 5-HT<sub>2</sub> and beta-adrenergic receptor binding sites in the brain of suicide victims. *Arch Gen Psychiatry* 47:1038–1047.
- Arango V, Underwood MD, McDevitt PJ, Gubbi AV, Mann JJ (1995): Localized alterations in pre- and postsynaptic serotonin binding sites in the ventrolateral prefrontal cortex of suicide victims. *Brain Res* 688:121–133.
- Arikuni T, Kubota K (1986): The organization of prefrontocaudate projections and their laminar origin in the macaque monkey: a retrograde study using HRP-gel. *J Comp Neurol* 244:492–510.
- Baxter LR, Schwartz JM, Phelps ME, Mazziotta JC, Guze BM, Selin CE, et al (1989): Reduction of prefrontal cortex glucose metabolism common to three types of depression. *Arch Gen Psychiatry* 46:243–250.
- Bench CJ, Friston KJ, Brown RG, Frackowiak RSJ, Dolan RJ (1993): Regional cerebral blood flow in depression measured by positron emission tomography: the relationship with clinical dimensions. *Psychol Med* 23:579–590.
- Biver F, Goldman S, Delvenne V, Luxen A, Maertelaer VD, Hubain P, et al (1994): Frontal and parietal metabolic disturbances in unipolar depression. *Biol Psychiatry* 36:381–388.
- Biver F, Wikler D, Lotstra F, Damhaut P, Goldman S, Mendlewicz J (1997): Serotonin 5-HT<sub>2</sub> receptor imaging in major depression: focal changes in orbito-insular cortex. *Br J Psychiatry* 171:444–448.
- Bremner JD, Innis RB, Salomon RM, Staib LH, Ng CK, Miller HL, et al (1997): Positron emission tomography measurement of cerebral metabolic correlates of tryptophan depletion-induced depressive relapse. *Arch Gen Psychiatry* 54:364–374.
- Buchsbaum MS, Wu J, Delisi LE, Holcomb H, Kessler R, Johnson J, et al (1986): Frontal cortex and basal ganglia metabolic rates assessed by positron emission tomography with [<sup>18</sup>F]-Deoxyglucose in affective illness. *J Affect Disord* 10:137–152.
- Coffey CE, Wilkinson WI, Weiner RD, Parashos IA, Djang WT, Webb MC, et al (1993): Quantitative cerebral anatomy in depression. *Arch Gen Psychiatry* 50:7–16.
- Drevets W, Price J, Simpson JR J, Todd R, Reich T, Vannier M, et al (1997): Subgenual prefrontal cortex abnormalities in mood disorders [see comments]. *Nature* 386:824–827.
- Drevets WC, Raichle ME (1992): Neuroanatomical circuits in depression: implications for treatment mechanisms. *Psychopharmacol Bull* 28:261–274.
- Drevets WC, Videen TO, Price JL, Preskorn SH, Carmichael T, Raichle ME (1992): A functional anatomical study of unipolar depression. *J Neurosci* 12:3628–3641.
- Goldman-Rakic PS (1998): The cortical dopamine system: role in memory and cognition. *Adv Pharmacol* 42:707–711.
- Goldman-Rakic PS, Lidow MS, Gallager DW (1990): Overlap of dopaminergic, adrenergic, and serotonergic receptors and complementarity of their subtypes in primate prefrontal cortex. *J Neurosci* 10:2125–2138.
- Gundersen HJG (1986): Stereology of arbitrary particles: a review of unbiased number and size estimators and the presentation of some new ones, in memory of William R. Thompson. *J Microscopy* 143:3–45.
- Heninger GR, Charney DS (1987): Mechanisms of action of antidepressant treatments: implications for the etiology and treatment of depressive disorders. In: Meltzer HY, editor. *Psychopharmacology: The Third Generation of Progress*. Raven Press.
- Hollister LE, Claghorn JL (1993): New antidepressants. *Annu Rev Pharmacol Toxicol* 33:165–177.
- Joyce JN, Janowsky A, Neve KA (1991): Characterization and distribution of [<sup>125</sup>I]epidepride binding to dopamine D<sub>2</sub> receptors in basal ganglia and cortex of human brain. *J Pharmacol Exp Therapeut* 257:1253–1263.
- Kelly TM, Mann JJ (1996): Validity of DSM-III-R diagnosis by psychological autopsy: a comparison with clinician ante-mortem diagnosis. *Acta Psychiatr Scand* 94:337–343.

- Klimek V, Stockmeier C, Overholser J, Meltzer H, Kalka S, Dilley G, et al (1997): Reduced levels of norepinephrine transporters in the locus coeruleus in major depression. *J Neurosci* 17:8451–8458.
- Koenderink MJ, Uylings HB, Mrzljak L (1994): Postnatal maturation of the layer III pyramidal neurons in the human prefrontal cortex: a quantitative Golgi analysis. *Brain Res* 653:173–182.
- Kostovic I, Skavic J, Strinovic D (1988): Acetylcholinesterase in the human frontal associative cortex during the period of cognitive development: early laminar shifts and late innervation of pyramidal neurons. *Neurosci Lett* 90:107–112.
- Lewis DA (1992): The catecholaminergic innervation of primate prefrontal cortex. *J Neural Transm* 36:179–200.
- Lewis DA, Morrison JH (1989): Noradrenergic innervation of monkey prefrontal cortex: a dopamine  $\beta$ -hydroxylase immunohistochemical study. *J Comp Neurol* 282:317–330.
- Mrzljak L, Uylings HBM, Kostovic I, van Eden CG (1992): Prenatal development of neurons in the human prefrontal cortex. II. A quantitative golgi study. *J Comp Neurol* 316:485–496.
- Öngür D, Drevets WC, Price JL (1998): Glial reduction in the subgenual prefrontal cortex in mood disorders. *Proc Natl Acad Sci USA* 95:13290–13295.
- Ordway GA, Widdowson PS, Smith KS, Halaris A (1994): Agonist binding to  $\alpha_2$ -adrenoceptors is elevated in the locus coeruleus from victims of suicide. *J Neurochem* 63:617–624.
- Pacheco MA, Stockmeier C, Meltzer HY, Overholser JC, Dilley GE, Jope RS (1996): Alterations in phosphoinositide signaling and G-protein levels in depressed suicide brain. *Brain Res* 723:37–45.
- Pazos A, Probst A, Palacios J (1987): Serotonin receptors in the human brain—III. Autoradiographic mapping of serotonin-1 receptors. *Neuroscience* 21:97–122.
- Rajkowska G (1997): Morphometric methods for studying the prefrontal cortex in suicide victims and psychiatric patients. *Ann NY Acad Sci* 836:253–268.
- Rajkowska G, Goldman-Rakic PS (1995a): Cytoarchitectonic definition of prefrontal areas in the normal human cortex: I: Quantitative criteria for distinguishing areas 9 and 46. *Cereb Cortex* 4:307–322.
- Rajkowska G, Goldman-Rakic PS (1995b): Cytoarchitectonic definition of prefrontal areas in the normal human cortex: II. Variability in locations of areas 9 and 46. *Cereb Cortex* 4:323–337.
- Rajkowska G, Pool CW, Roland PE, Zilles K, Uylings H (1998a): 3-D cytoarchitectonic parcellation of human orbitofrontal cortex. Correlation with postmortem MRI. *Soc Neurosci Abstr* 24:165.
- Rajkowska G, Selemon L, Goldman-Rakic P (1998b): Neuronal and glial somal size in the prefrontal cortex: a postmortem morphometric study of schizophrenia and Huntington's disease. *Arch Gen Psychiatry* 55:215–224.
- Rajkowska G, Selemon LD, Goldman-Rakic PS (1997): Marked glial neuropathology in prefrontal cortex distinguishes bipolar disorder from schizophrenia. *Schizophrenia Res* 24:41.
- Robinson RG, Szetela B (1981): Mood changes following left hemispheric brain injury. *Ann Neurol* 9:447–453.
- Schwartz ML, Goldman-Rakic PS (1984): Callosal and intra-hemispheric connectivity of the prefrontal association cortex in rhesus monkey: relation between intraparietal and principal sulcal cortex. *J Comp Neurol* 226:403–420.
- Selemon LD, Goldman-Rakic PS (1985): Longitudinal topography and interdigitation of corticostriatal projections in the rhesus monkey. *J Neurosci* 5:776–794.
- Selemon LD, Goldman-Rakic PS (1988): Common cortical and subcortical target areas of the dorsolateral prefrontal and posterior parietal cortices in the rhesus monkey: Evidence for a distributed neural network subserving spatially guided behavior. *J Neurosci* 8:4049–4068.
- Selemon LD, Rajkowska G, Goldman-Rakic PS (1995): Abnormally high neuronal density in the schizophrenic cortex: a morphometric analysis of prefrontal area 9 and occipital area 17. *Arch Gen Psychiatry* 52:805–818.
- Smiley J, Goldman-Rakic P (1996): Serotonergic axons in monkey prefrontal cerebral cortex synapse predominantly on interneurons as demonstrated by serial section electron microscopy. *J Comp Neurol* 367:431–443.
- Spitzer R, Endicott J (1978): Schedule for affective disorders and schizophrenia (SADS), Third Edition. New York: New York State Psychiatric Institute.
- Steingard R, Renshaw P, Yurgelun-Todd D, Wald L (1998): Proton MRS studies of the orbitofrontal cortex of depressed adolescents. *Biol Psychiatry* 43:28S.
- Stockmeier C, Shapiro L, Dilley G, Kolli T, Friedman L, Rajkowska G (1998): Increase in serotonin-1A autoreceptors in the midbrain of suicide victims with major depression—postmortem evidence for decreased serotonin activity. *J Neurosci* 18:7394–7401.
- Tsacopoulos M, Magistretti PJ (1996): Metabolic coupling between glia and neurons. *J Neurosci* 16:877–885.
- Williams RW (1989): Three-dimensional counting: an accurate and direct method to estimate numbers of cells in sectioned material. (Erratum). *J Comp Neurol* 281:335.
- Williams RW, Rakic P (1988): Three-dimensional counting: an accurate and direct method to estimate numbers of cells in sectioned material. *J Comp Neurol* 278:344–352.
- Williams SM, Goldman-Rakic PS (1998): Widespread origin of the primate mesofrontal dopamine system. *Cereb Cortex* 8:321–345.